

CHIRAL DYNAMICS IN $\gamma p \rightarrow \pi^0 \eta p$ AND RELATED REACTIONS¹M. Döring^{2*}, E. Oset^{3*}, D. Strottman^{4*,†}^{*}Departamento de Física Teórica and IFIC, Centro Mixto Universidad de Valencia-CSIC, Institutos de Investigación de Paterna, Aptd. 22085, 46071 Valencia, Spain[†]Theoretical Division, Los Alamos National Laboratory, Los Alamos, NM 87545, USA

Received 3 November 2005, in final form 24 November 2005, accepted 28 November 2005

Using a chiral unitary approach for meson-baryon scattering in the strangeness zero sector, where the $N^*(1535)$ and $\Delta^*(1700)$ resonances are dynamically generated, we study the reactions $\gamma p \rightarrow \pi^0 \eta p$ and $\gamma p \rightarrow \pi^0 K^0 \Sigma^+$ at photon energies at which the final states are produced close to threshold. Among several reaction mechanisms, we find the most important is the excitation of the $\Delta^*(1700)$ state which subsequently decays into a pseudoscalar meson and the $N^*(1535)$. Hence, the reaction provides useful information with which to test current theories of the dynamical generation of the low-lying $1/2^-$ and $3/2^-$ states. Predictions are made for cross sections and invariant mass distributions which can be compared with forthcoming experiments at ELSA.

PACS: 25.20.Lj, 11.30.Rd

1 Introduction

The unitary extensions of chiral perturbation theory $U\chi PT$ have brought new light in the study of the meson-baryon interaction and have shown that some well known resonances qualify as dynamically generated, the properties of which are described in terms of chiral Lagrangians. After early studies in this direction explaining the $\Lambda(1405)$ and the $N^*(1535)$ as dynamically generated resonances [1–5], more systematic studies have shown that there are two octets and one singlet of resonances from the interaction of the octet of pseudoscalar mesons with the octet of stable baryons [6, 7]. The $N^*(1535)$ belongs to one of these two octets and plays an important role in the πN interaction with its coupled channels ηN , $K\Lambda$ and $K\Sigma$ [8]. Here, we adopt and extend the ideas of Ref. [9] for the reaction $\gamma p \rightarrow K^+ \pi \Sigma$ and study the analogous reaction $\gamma p \rightarrow \pi^0 \eta p$ where the ηp final state can form the $N^*(1535)$ resonance. Besides processes relevant in $\gamma p \rightarrow \pi \pi N$ [10], we also include [11] the contribution from the $\Delta^*(1700)$ resonance which qualifies as dynamically generated through the interaction of the 0^- meson octet and the $3/2^+$ baryon decuplet as recent studies show [12, 13].

¹Presented at the Workshop on Production and Decay of η and η' Mesons (ETA05), Cracow, 15–18 September 2005.²E-mail address: doering@ific.uv.es³E-mail address: oset@ific.uv.es⁴E-mail address: dds@ific.uv.es

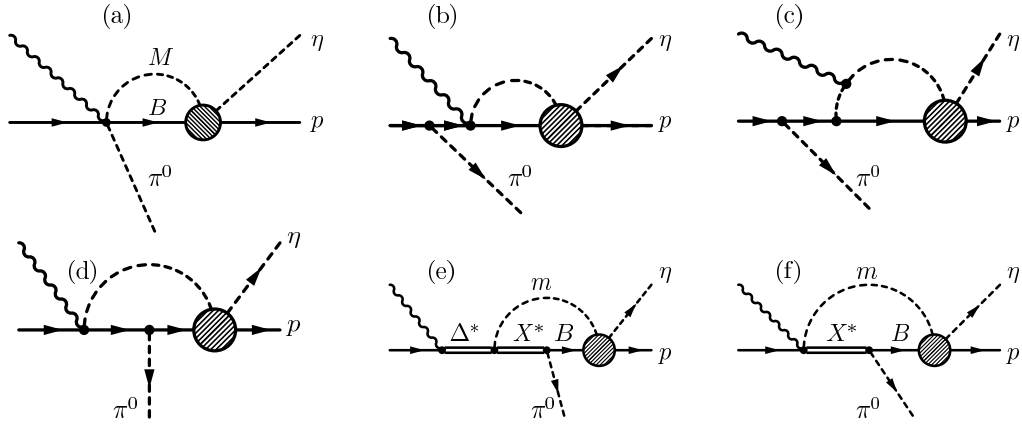


Fig. 1. Photoproduction mechanisms for the $\pi^0\eta p$ final state.

At the same time we also study the $\gamma p \rightarrow \pi^0 K^0 \Sigma^+$ reaction and make predictions for its cross section, taking advantage of the fact that it appears naturally within the coupled channels formalism of the $\gamma p \rightarrow \pi^0 \eta p$ reaction and leads to a further test of consistency of the ideas explored here. Both reactions are currently being analyzed at ELSA [14].

2 Eta pion photoproduction

Before turning to the two-meson photoproduction, we give a short review of the properties of the $N^*(1535)$ in the meson-baryon sector, where this resonance shows up clearly in the spin isospin ($S = 1/2, I = 1/2$) channel. The model of Ref. [8] provides an accurate data description of elastic and quasielastic πN scattering in the S_{11} channel. Within the coupled channel approach in the $SU(3)$ representation of Ref. [8], not only the πN final state is accessible, but also $K\Sigma$, $K\Lambda$, and ηN in a natural way. In Ref. [11] it is shown that the same model for the resonance provides a good data description close to threshold for the one- η photoproduction, $\gamma p \rightarrow \eta p$, when including some basic photoproduction mechanisms, which makes us confident to use the model of the $N^*(1535)$ for the more complex reaction with two mesons in the final state in the next section.

2.1 Production mechanisms for $\gamma p \rightarrow \pi^0 \eta p$

In Fig. 1 some photoproduction mechanisms are shown. Diagrams (c) shows the pole terms that accompanies the contact term (b) in order to ensure gauge invariance. Similar terms are included for diagrams (a), (d), and (f) but not separately drawn. A π^0 emission from the last proton gives small amplitudes as discussed in Ref. [11]. In addition, photon couplings to the bubbles implicit in the dashed circles of Fig. 1 would vanish for parity reasons or would be very small. In all diagrams, the gray blob signifies the dynamically generated $N^*(1535)$ that provides the final state interaction $MB \rightarrow \eta p$ with the intermediate meson-baryon state in the loop given by the

list of channels from above. Here, we can only give a qualitative description of the processes and the amplitudes which are denoted in detail in Ref. [11].

Diagram (a) uses a contact term in a similar way as for the $K^+ \Lambda(1405)$ photoproduction in Ref. [9], additionally taking into account the anomalous magnetic moment of the nucleon with the effective Lagrangian from Ref. [18]. Diagrams (b) and (c) are a straightforward extension of the basic photoproduction mechanisms in $\gamma p \rightarrow \eta p$ [11] for the final state with an additional π^0 . It is known that the inclusion of explicit resonances plays an important role in the two-pion photoproduction [10], and therefore we include the relevant mechanisms as sub-processes in the calculation: In diagram (e) we show the contribution from the $\Delta^*(1700)$ decay into $X^* = \Delta(1232)$ and $m = \pi$. In the same way, the $N^*(1520)$ decay from Ref. [10] is taken into account. Fig. (f) shows the corresponding Δ -Kroll-Ruderman term ($X^* = \Delta, m = \pi, B = N$) and also the Σ^* -Kroll-Ruderman term ($X^* = \Sigma^*, m = K, B = \Lambda$). Additionally, we include the contribution from the dynamically generated $3/2^-$ resonance from Ref. [13] which has been identified with the $\Delta^*(1700)$. Here, we treat it explicitly but take its couplings from the chiral theory. In particular, the decay channels (mX^*B) = ($\eta\Delta^+(1232)p$), ($K^+\Sigma^{*0}(1385)\Lambda$), ($K^0\Sigma^{*+}\Sigma^+$) in diagram (e) are possible, whose strengths are not measured yet in experiment but a genuine prediction of the model [13]. From these couplings, also a tree level diagram originates for the photoproduction: $\gamma p \rightarrow \Delta^*(1700) \rightarrow \eta\Delta^+(1232)[\pi^0 p]$ which gives the largest contribution. The widths of the resonances are taken into account [11]. There are no free parameters in the theory once the low energy constants of the $N^*(1535)$ are fitted in the $\pi N \rightarrow \pi N$ reaction [8] and the regularization of the first loop of the processes in Fig. 1 in the $\gamma p \rightarrow \eta p$ reaction [11].

3 Numerical results

The invariant mass spectra for $M_I(\eta p)$ and $M_I(\pi^0 p)$ and cross section for the $\gamma p \rightarrow \pi^0 \eta p$ reaction are predicted which can be directly compared to the forthcoming experiments at the ELSA facility. In Fig. 2 the spectrum for $M_I(\eta p)$ is shown for several lab photon energies E_γ , taking into account all processes from Fig. 1 plus the tree level process described at the end of Sec. 2.1. The solid and dashed curves correspond to the full and reduced model (no $\pi N \rightarrow \pi \pi N$ channel, no vector exchange in t -channel, see Ref. [8], [11]) for the $N^*(1535)$ resonance, and we take the difference as a hint for the theoretical error although at higher energies it could be larger. The $N^*(1535)$ is clearly visible in the spectrum, although it interferes with the tree level process at low E_γ which shifts its position slightly. At higher E_γ , we observe a second peak which moves with the energy. This is a reflection of the $\Delta(1232)$ in the tree level process which is on shell around these invariant masses. For a more detailed discussion, see Ref. [11]. The $\pi^0 p$ invariant mass spectrum is not shown here, but in Ref. [11]. There, the $\Delta(1232)$ shows up as a clean signal as expected. The total cross section is plotted in Fig. 3. Additionally to the full and reduced model, we show the outcome when using the phenomenological meson-baryon $\rightarrow \eta p$ transition from the PWA from Ref. [19]. From the processes with $N^*(1535)$, diagram (e) from Fig. 1 with $m = \eta, X^* = \Delta(1232)$ gives the largest contribution which is due to the strong $\eta p \rightarrow \eta p$ transition in the model for the $N^*(1535)$. Also, the tree level diagram contributes significantly as we have already seen in Fig. 2. The cross section is relatively independent of the chosen model for the $N^*(1535)$ (solid vs. dashed line), and even the the phenomenological potential does not change much the result.

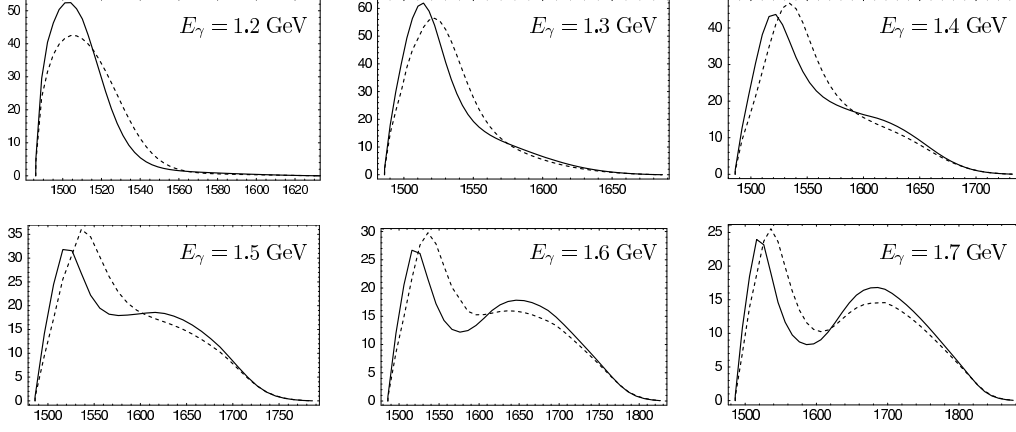


Fig. 2. Invariant mass spectrum $\frac{d\sigma}{dM_I(\eta p)}$ [$\mu\text{b GeV}^{-1}$] as a function of $M_I(\eta p)$ [MeV] for various photon lab energies E_γ . Solid and dashed lines: Full and reduced model for the $N^*(1535)$, respectively.

The $\gamma p \rightarrow \pi^0 K^0 \Sigma^+$ reaction is calculated in a similar way as for the $\pi^0 \eta p$ final state by replacing the ηp final state of the $N^*(1535)$ by the $K^0 \Sigma^+$ one and including a new tree level diagram in analogy to the process described at the end of Sec. 2.1: $\gamma p \rightarrow \Delta^{*+}(1700) \rightarrow K^0 \Sigma^{*+} [\pi^0 \Sigma^+]$. The cross section for $\gamma p \rightarrow \pi^0 K^0 \Sigma^+$ is much smaller than for the $\pi^0 \eta p$ final state as Fig. 3 shows. This is — among other reasons [11] — due to the fact that the reaction takes place at much higher photon energies where the dynamically generated $N^*(1535)$ is off shell.

4 Conclusions

In this paper we have studied the reactions $\gamma p \rightarrow \pi^0 \eta p$ and $\gamma p \rightarrow \pi^0 K^0 \Sigma^+$ within a chiral unitary framework which considers the interaction of mesons and baryons in coupled channels and dynamically generates the $N^*(1535)$. From the various processes, we find dominant the decay of the dynamically generated $\Delta^*(1700)$ resonance into $\eta \Delta$, followed by the unitarization, or in other words, the $\Delta^*(1700) \rightarrow \pi^0 N^*(1535)$ decay. A similar term provides also a tree level process which leads, together with the $N^*(1535)$, to a characteristic double hump structure in the ηp and $\pi^0 p$ invariant masses at higher photon energies.

Although we have used the $\Delta^*(1700)$ explicitly in the model, its couplings are taken from the chiral theory where it appears dynamically generated and the experiment would be indirectly testing such couplings.

The measurement of both cross sections is being performed at the ELSA/Bonn Laboratory and hence the predictions are both interesting and opportune and can help us gain a better insight in the nature of some resonances, particularly the $N^*(1535)$ and the $\Delta^*(1700)$ in the present case.

Acknowledgement: This work is partly supported by DGICYT contract number BFM2003-

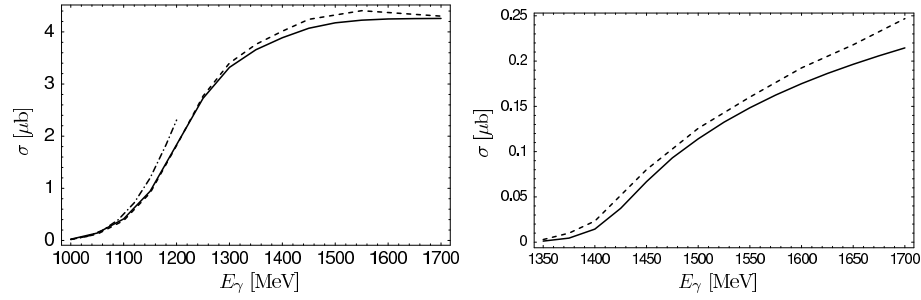


Fig. 3. Left side: Integrated cross section σ for the $\gamma p \rightarrow \pi^0 \eta p$ reaction. Right side: σ for the $\gamma p \rightarrow \pi^0 K^0 \Sigma^+$ reaction. Solid line: Full model for the $N^*(1535)$. Dashed line: Reduced model. Dashed dotted line (left side): Phenomenological potential for the $MB \rightarrow \eta p$ transition (only available up to $E_\gamma \sim 1.2$ GeV).

00856, and the E.U. EURIDICE network contract no. HPRN-CT-2002-00311. This research is part of the EU Integrated Infrastructure Initiative Hadron Physics Project under contract number RII3-CT-2004-506078.

References

- [1] N. Kaiser, P. B. Siegel, W. Weise: *Phys. Lett. B* **362** (1995) 23
- [2] N. Kaiser, T. Waas, W. Weise: *Nucl. Phys. A* **612** (1997) 297
- [3] E. Oset, A. Ramos: *Nucl. Phys. A* **635** (1998) 99
- [4] J. C. Nacher, A. Parreno, E. Oset, A. Ramos, A. Hosaka, M. Oka: *Nucl. Phys. A* **678** (2000) 187
- [5] J. A. Oller, U. G. Meissner: *Phys. Lett. B* **500** (2001) 263
- [6] D. Jido, J. A. Oller, E. Oset, A. Ramos, U. G. Meissner: *Nucl. Phys. A* **725** (2003) 181
- [7] C. Garcia-Recio, M. F. M. Lutz, J. Nieves: *Phys. Lett. B* **582** (2004) 49
- [8] T. Inoue, E. Oset, M. J. Vicente Vacas: *Phys. Rev. C* **65** (2002) 035204
- [9] J. C. Nacher, E. Oset, H. Toki, A. Ramos: *Phys. Lett. B* **455** (1999) 55
- [10] J. C. Nacher, E. Oset, M. J. Vicente, L. Roca: *Nucl. Phys. A* **695** (2001) 295
- [11] M. Doring, E. Oset, D. Strottman: arXiv:nucl-th/0510015
- [12] E. E. Kolomeitsev, M. F. M. Lutz: *Phys. Lett. B* **585** (2004) 243
- [13] S. Sarkar, E. Oset, M. J. Vicente Vacas: *Nucl. Phys. A* **750** (2005) 294
- [14] V. Metag, M. Nanova: private communication
- [15] J. Gasser, H. Leutwyler: *Nucl. Phys.* **B250** (1985) 465, 517, 539
- [16] U. G. Meissner: *Rep. Prog. Phys.* **56** (1993) 903; V. Bernard, N. Kaiser, U. G. Meissner: *Int. J. Mod. Phys. E* **4** (1995) 193
- [17] G. Ecker: *Prog. Part. Nucl. Phys. E* **35** (1995) 1
- [18] D. Jido, A. Hosaka, J. C. Nacher, E. Oset, A. Ramos: *Phys. Rev. C* **66** (2002) 025203
- [19] R. A. Arndt, W. J. Briscoe, I. I. Strakovsky, R. L. Workman, M. M. Pavan: *Phys. Rev. C* **69** (2004) 035213